Electronic Supplementary Information

Convenient Multicomponent Synthesis of Furo[3,2-*C*]Coumarins in Promoting Medium DIPEAc and assessment of their therapeutic potential through *in silico* pharmacophore based target screening

Shabnam M. Shaikh,[a†]Vinay K. Yadav,[b†] Ghanshyam Mali,[c†] Giribala M. Bondle,[a] Akhilesh Kumar,[d] Rohan D. Erande,[c*] Sudipta Bhattacharyya,[b*] and Manisha R. Bhosle,[a*]

[a]Department of Chemistry, Dr. B. A. M. University, Aurangabad 431004, Maharashtra, India

[b]Department of Bioscience & Bioengineering, Indian Institute of Technology Jodhpur, Jodhpur 342037, Rajasthan, India

[c]Department of Chemistry, Indian Institute of Technology Jodhpur, Jodhpur 342037, Rajasthan, India

[d]Department of Chemistry, Indian Institute of Technology Kanpur, Kanpur 208016, India

Table of contents

Experimental

General

All the chemicals were purchased from S. D. Fine, Sigma-Aldrich or Merck and used as received. Melting points of all the synthesized compounds were determined in open capillary tubes and are uncorrected. ^{1}H NMR spectra were recorded with a Bruker Avance 400 spectrometer operating at 400 and 500 MHz using $CDCl_3$ and DMSO solvent and tetramethylsilane (TMS) as the internal standard and chemical shift in δ ppm. Mass spectra were recorded on a Sciex, Model; API 3000 LCMS/MS Instrument. The purity of each compound was checked by TLC using silica-gel, $60F_{254}$ aluminum sheets as adsorbent and visualization was accomplished by iodine/ultraviolet light.

General procedure for the synthesis of trans-2-(substituted benzoyl)-3-(4-substituted phenyl)-2H-furo[3,2-c]chromen-4(3H)-ones (4a-t)

To a stirred solution of α-bromo acetyl substrate (phenacyl bromide or 2-bromoacetophenone) (4 mmol) in DIPEAc (3ml) was added aldehyde (4 mmol) followed by 4-hydroxy-2H-chromen-2-one (4 mmol). Then the resulting reaction mixture was stirred at 80 ^{o}C for 1 hr after the completion of reaction (monitored by TLC), the reaction mixture was cooled at room temperature and diluted with cold water. The solid separated was collected by filtration at pump. The products were purified by crystallization in ethanol. The compounds were characterized by ^{1}HNMR, ^{13}CNMR and Mass spectroscopy and are in good agreement with those reported in the literature.[1,2]

General procedure for the synthesis of diisopropylethylammonium acetate (DIPEAc)

A mixture of glacial acetic acid (0.02 mol) and N-ethyl-N-isopropylpropan-2-amine (0.02 mol) was stirred at 0-10 °C for 30 min to obtain DIPEAc as a viscous liquid.

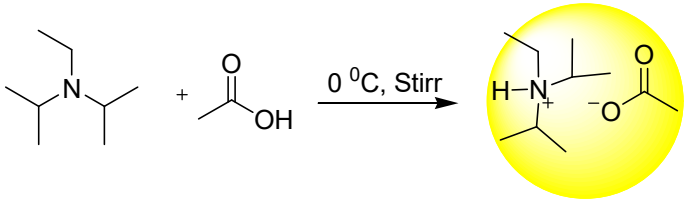

Scheme 1 Synthesis of diisopropylethylammonium acetate (DIPEAc)

Spectral Data

FTIR of *N,N*-diisopropylethyl ammonium acetate (DIPEAc)

FTIR (υ^{-cm}, ATR): 2984, 2492, 1960, 1711, 1562, 1393, 1360, 1247, 1180, 1132, 1097, 1071, 1005, 932, 875, 809, 781, 729, 655, 613.

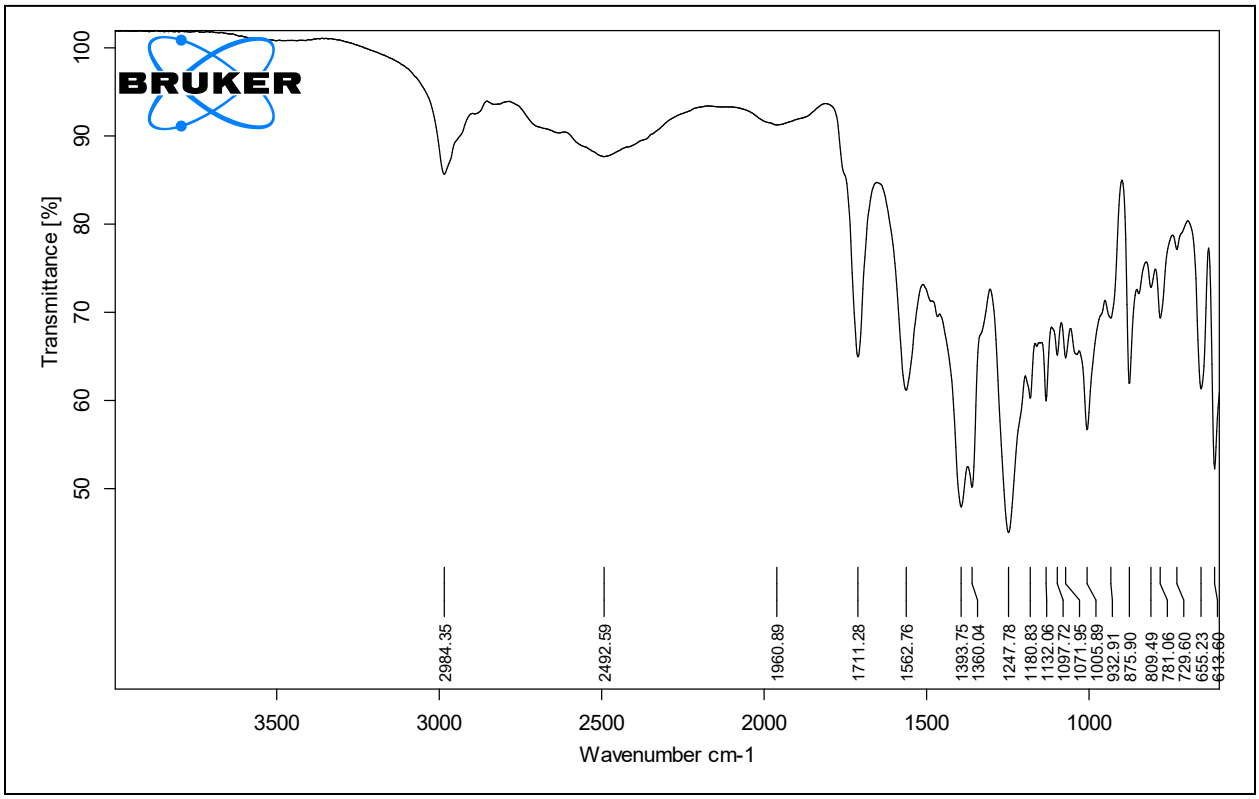

2-Benzoyl-3-phenyl-2H-furo[3,2-c]chrome-4(3H)-one (4a)

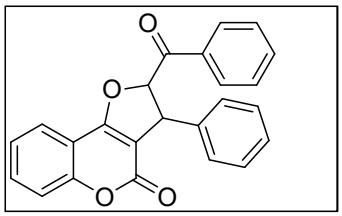

^{1}HNMR (400 MHz, $CDCl_3$ ∂ ppm): 7.65 - 7.88 (m, 7H, Ar-H), 7.41-7.54 (m, 7H, Ar-H),6.180 (s, 1H, CH), 4.80 (s, 1H, CH); ^{13}CNMR (100 MHz, $CDCl_3$ ∂ ppm): 192.30, 166.56, 159.46, 155.64, 139.78, 134.62, 133.43, 133.11, 129.50, 129.30, 129.23, 128.37, 127.76, 124.34, 123.41, 117.27, 112.41, 105.58, 92.87, 49.58; LC-MS (ESI, m/e): 369.0 [M^+].

2-(4-Chlorobenzoyl)-3–phenyl-2H–furo [3,2-c] chromen-4(3H)-one (4b)

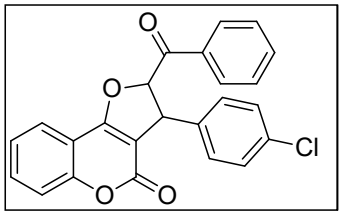

^{1}HNMR (400 MHz, $CDCl_3$ ∂ ppm: 4.81 (s, 1H, CH), 6.104 (s, 1H, CH), 7.237-7.25 (m, 5H, Ar-H), 7.59 -7.8 (m, 4H, Ar-H), 7.7- 7.8 (m, 4H, Ar-H); ^{13}CNMR (100 MHz, $CDCl_3$ ∂ ppm): 191.46, 167.28, 165.75, 160.21, 156.73, 140.86, 134.72, 132.39, 131.97, 128.99, 128.27, 127.69, 127.11, 126.47, 125.32, 123.80, 116.89, 114.48, 112.90, 106.27, 92.50, 49.81; LC-MS (ESI, m/e): 403.05 [M^+]

2-Benzoyl-3-(4-methoxyphenyl)-2H-furo[3,2-c]chromen-4(3H)-one (4c)

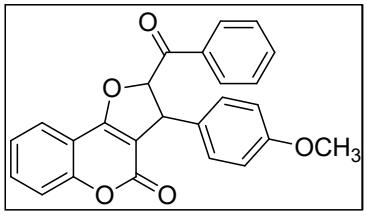

^{1}HNMR (400 MHz, $CDCl_3$ ∂ ppm): 7.82-7.89 (m, 3H), 7.60-7.62 (m, 1H), 7.25-7.59 (m, 7H), 6.94-6.97 (m, 2H), 4.81 (s, 1H), 4.79 (s, 1H), 3.70 (s, 3H); ^{13}CNMR (100 MHz, $CDCl_3$ ∂ ppm): 190.78, 166.62, 164.75, 159.53, 155.63, 139.94, 133.04, 131.67, 131.19, 129.46, 128.30, 127.80, 127.07, 126.34, 124.30, 123.41, 117.24, 114.49, 112.46, 105.60, 92.72, 55.82, 49.75; LC-MS (ESI, m/e): 399.4 [M^+]

2-Benzoyl-3-(4-fluorophenyl)-2H-furo[3,2-c]chromen-4(3H)-one (4f)

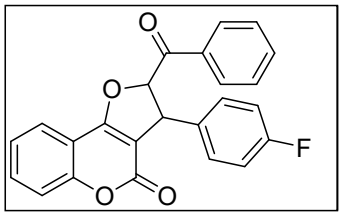

^{1}HNMR (400 MHz, $CDCl_3$ ∂ ppm): 7.81-7.91 (m, 2H), 7.53-7.68 (m, 4H), 7.30-7.50 (m, 5H), 7.03-7.29 (m, 2H), 6.11-6.68 (m, 1H), 4.81-4.83 (m, 1H); ^{13}CNMR (100 MHz, $CDCl_3$ ∂ ppm):

192.16, 166.54, 164.36, 161.09, 159.42, 155.65, 135.54, 134.71, 133.46, 130.52, 129.51, 129.40, 128.99, 124.41, 123.41, 117.31, 116.29, 115.56, 112.31, 105.36, 32.79, 48.78; LC-MS (ESI, m/e): 387.2 [M^+]

2-(4-Hydroxybenzoyl)-3–phenyl-2H–furo [3,2-c] chromen-4(3H)-one (4h)

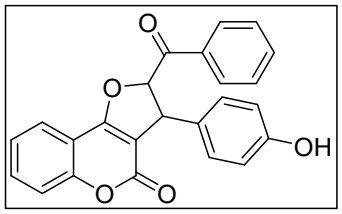

^{1}H NMR (500 MHz, $CDCl_3$+DMSO-d_6) δ 9.09 (d, *J*=12.5 Hz, 1H), 7.83 (s, 3H), 7.60 (d, *J* = 7.2 Hz, 2H), 7.46 (d, *J* = 5.7 Hz, 2H), 7.32 (d, *J* = 3.2 Hz, 2H), 7.07-6.94 (m, 2H), 6.79-6.66 (m, 2H), 6.22-6.08 (m, 1H), 4.53 (d, *J*=4.6 Hz, 1H);**^{13}C NMR** (126 MHz, $CDCl_3$+DMSO-d_6) δ 192.46, 166.19, 159.10, 157.39, 155.19, 134.48, 133.03, 129.99, 129.65, 129.07, 128.60, 124.32, 123.23, 116.85, 116.18, 115.13, 112.15, 105.31, 92.79, 48.83; **HRMS:** m/z (chemical formula $C_{24}H_{16}O_5$) cal. $[M]^+$: 384.0992, found: 384.0957; cal. $[M+H]^+$: 385.1071, found: 385.1090.

2-(3-Hydroxybenzoyl)-3–phenyl-2H–furo [3,2-c] chromen-4(3H)-one (4j)

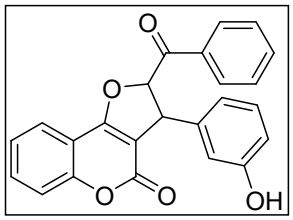

^{1}H NMR (500 MHz, $CDCl_3$+DMSO-d_6) δ 9.00 (s, 1H), 7.88-7.73 (m, 3H), 7.57 (ddt, *J*=7.1, 4.9, 4.2 Hz, 2H), 7.44 (td, *J* = 7.7, 4.3 Hz, 2H), 7.35-7.26 (m, 2H), 7.11 (td, *J* = 7.9, 3.6 Hz, 1H), 6.78-6.65 (m, 3H), 6.18-6.11 (m, 1H), 4.59 (t, *J*=3.8 Hz, 1H); **^{13}C NMR** (126 MHz, $CDCl_3$+DMSO-d_6) δ 192.23, 166.39, 159.18, 158.12, 155.22, 149.51, 140.90, 134.48, 133.02, 130.20, 129.07, 124.28, 123.93, 123.21, 118.41, 116.86, 115.49, 114.49, 112.11, 105.16, 92.51, 49.15; **HRMS:** m/z (chemical formula $C_{24}H_{16}O_5$) cal. $[M]^+$: 384.0992, found: 384.0942; cal. $[M+H]^+$: 385.1071, found: 385.1073.

2-(4-Bromobenzoyl)-3-phenyl-2H-furo[3,2-c]chromen-4(3H)-one (4o)

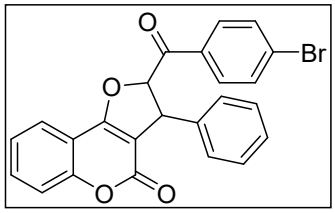

^{1}H NMR (500 MHz, $CDCl_3$) δ 7.85-7.75 (m, 3H), 7.67-7.58 (m, 3H), 7.41-7.29 (m, 7H), 6.10 (d, *J* = 5.0 Hz, 1H), 4.81 (d, *J* = 5.0 Hz, 1H);**^{13}C NMR** (126 MHz, $CDCl_3$) δ 191.36, 166.30, 159.33, 155.53, 139.50, 133.14, 132.55, 132.08, 130.66, 130.07, 129.51, 128.42, 127.67, 124.34, 123.27, 117.23, 112.20, 105.43, 92.68, 49.31; **HRMS:** m/z (chemical formula $C_{24}H_{15}BrO_4$) cal. $[M]^+$: 448.0131, found: 448.0087;cal.$[M+H-H_2O]^+$: 431.0104, found: 431.0124.

2-(4-Bromobenzoyl)-3-(4-hydroxyphenyl)-2H-furo[3,2-c]chromen-4(3H)-one (4p)

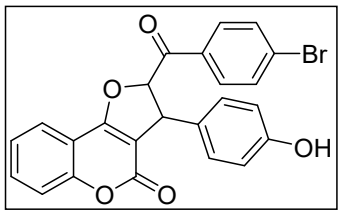

^{1}H NMR (500 MHz, $CDCl_3$+DMSO-d_6) δ 8.86 (s, 1H), 7.65 (dd, *J*=7.8, 1.4 Hz, 1H), 7.62-7.57 (m, 2H), 7.50-7.43 (m, 3H), 7.20 (dd, *J* = 8.1, 3.2 Hz, 2H), 6.91 (d, *J* = 8.5 Hz, 2H), 6.66 (d, *J* = 8.5 Hz, 2H), 5.94 (d, *J* = 5.0 Hz, 1H), 4.46 (d, *J* = 5.0 Hz, 1H);**^{13}C NMR** (126 MHz, $CDCl_3$+DMSO-d_6) δ 191.43, 165.89, 159.07, 157.27, 155.10, 132.83, 132.22, 131.77, 130.42, 129.64, 128.44, 124.13, 123.04, 116.77, 116.17, 115.21, 111.98, 105.23, 92.62, 48.62; **HRMS**: m/z (chemical formula $C_{24}H_{15}BrO_5$) cal.$[M-H2O]^+$: 445.9975, found: 445.9998.

3-(4-Hydroxyphenyl)-2-(4-methylbenzoyl)-2H-furo[3,2-c]chromen-4(3H)-one (4r)

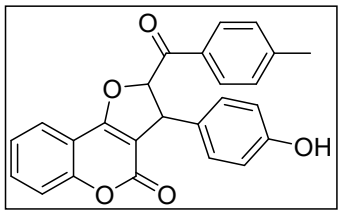

^{1}H NMR (500 MHz, DMSO-d_6+$CDCl_3$) δ 9.14 (s, 1H), 7.76 (dd, *J*=8.0, 1.5 Hz, 1H), 7.73-7.69 (m, 2H), 7.58 (dd, *J*=10.8, 5.0 Hz, 1H), 7.32 (dd, *J*=9.8, 4.5 Hz, 2H), 7.24 (d, *J* = 8.1 Hz, 2H), 6.99 (d, *J* = 8.4 Hz, 2H), 6.73 (d, *J* = 8.4 Hz, 2H), 6.14 (t, *J*=5.1 Hz, 1H), 4.48 (d, *J*=4.8 Hz, 1H), 2.37 (s, 3H); **^{13}C NMR** (126 MHz, DMSO) δ 192.06, 166.23, 159.04, 157.39, 155.18, 145.48, 133.05, 130.58, 130.07, 129.76, 129.19, 128.63, 124.35, 123.24, 116.84, 116.14, 112.17, 105.29, 92.71, 48.92, 21.84; **HRMS**: m/z (chemical formula $C_{25}H_{18}O_5$) cal. $[M+H]^+$: 401.1289, found: 401.1287.

3-(4-Hydroxyphenyl)-2-(4-methoxybenzoyl)-2H-furo[3,2-c]chromen-4(3H)-one (4t)

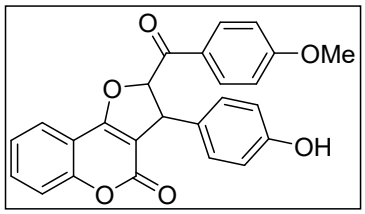

^{1}H NMR (500 MHz, $CDCl_3$) δ 8.81 (s, 1H), 7.65 (t, *J*=8.1 Hz, 3H), 7.45-7.36 (m, 1H),7.16 (t, *J* = 8.2 Hz, 2H), 6.89 (d, *J*=7.7 Hz, 2H), 6.77 (d, *J*=8.4 Hz, 2H), 6.63 (d, *J*=7.4 Hz, 2H), 5.92 (d, *J* = 4.0 Hz, 1H), 4.42 (d, *J* = 4.1 Hz, 1H), 3.78 – 3.59 (m, 3H);**^{13}C NMR** (126 MHz, $CDCl_3$) δ 190.71, 166.10, 164.34, 157.12, 155.07, 132.70, 131.25, 130.02, 128.42, 127.62, 125.77, 124.03, 123.06, 116.69, 116.05, 114.13, 112.07, 105.26, 92.50, 55.51, 48.95; **HRMS**: m/z (chemical formula $C_{25}H_{18}O_6$) cal.$[M+H]^+$: 415.1176, found: 415.1180.

[1]HNMR of Compound (4a)

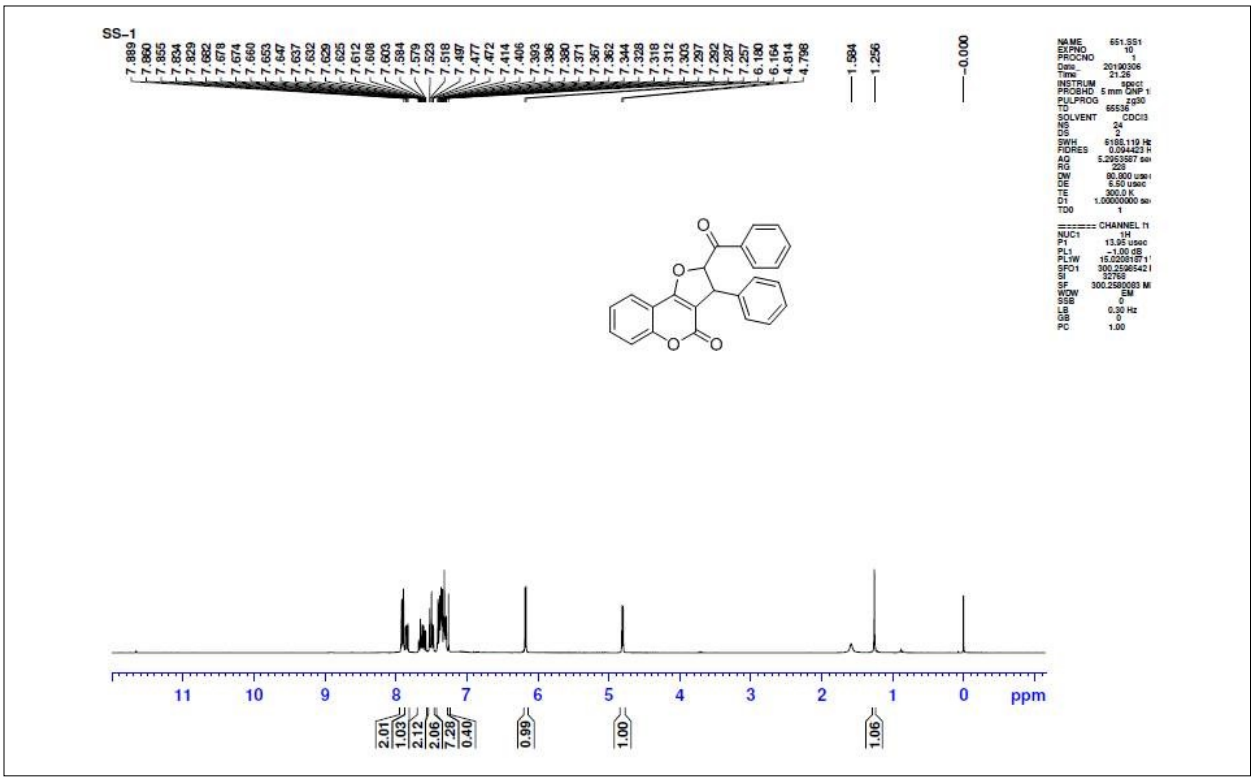

[13]CNMR of Compound (4a)

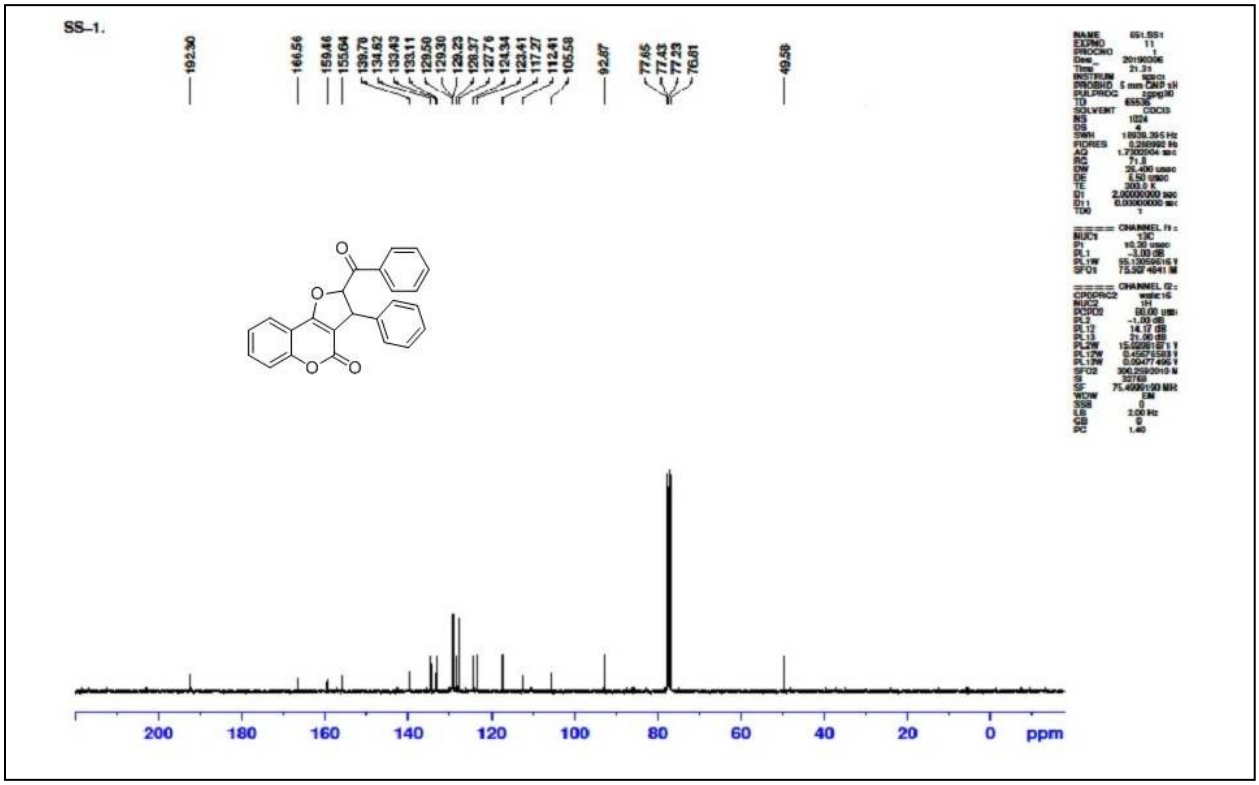

[1]HNMR of Compound (4b)

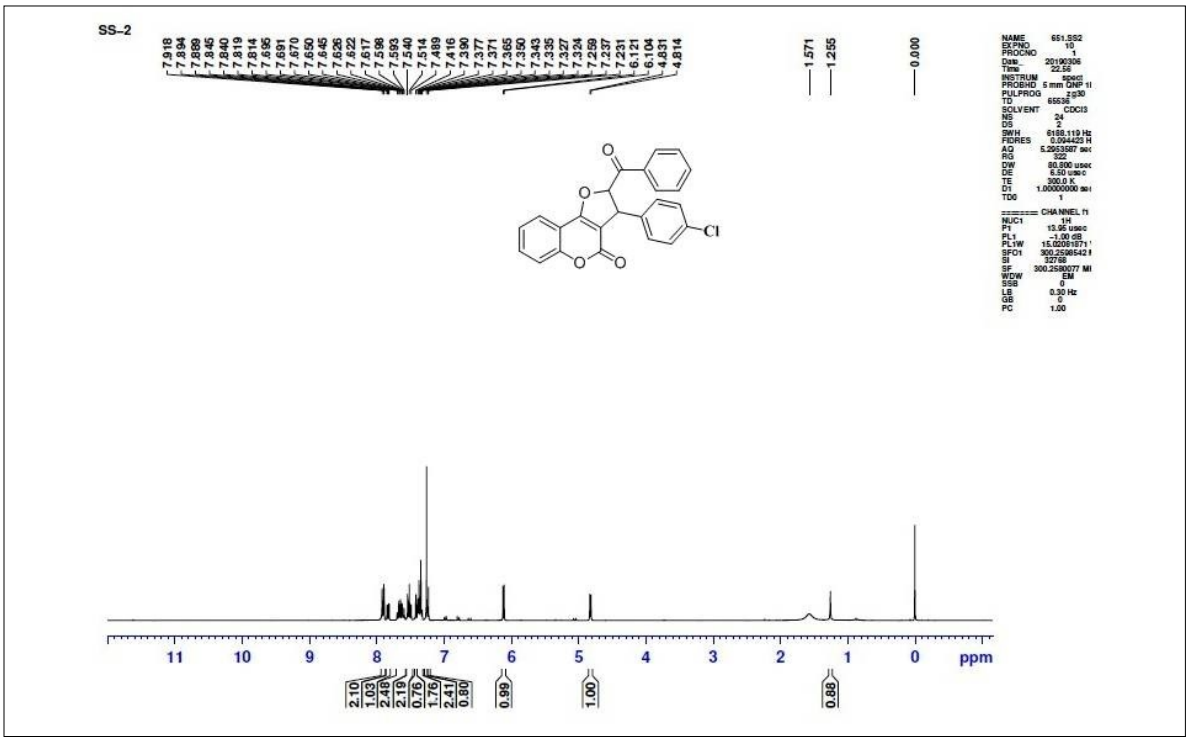

[1]HNMR of Compound (4c)

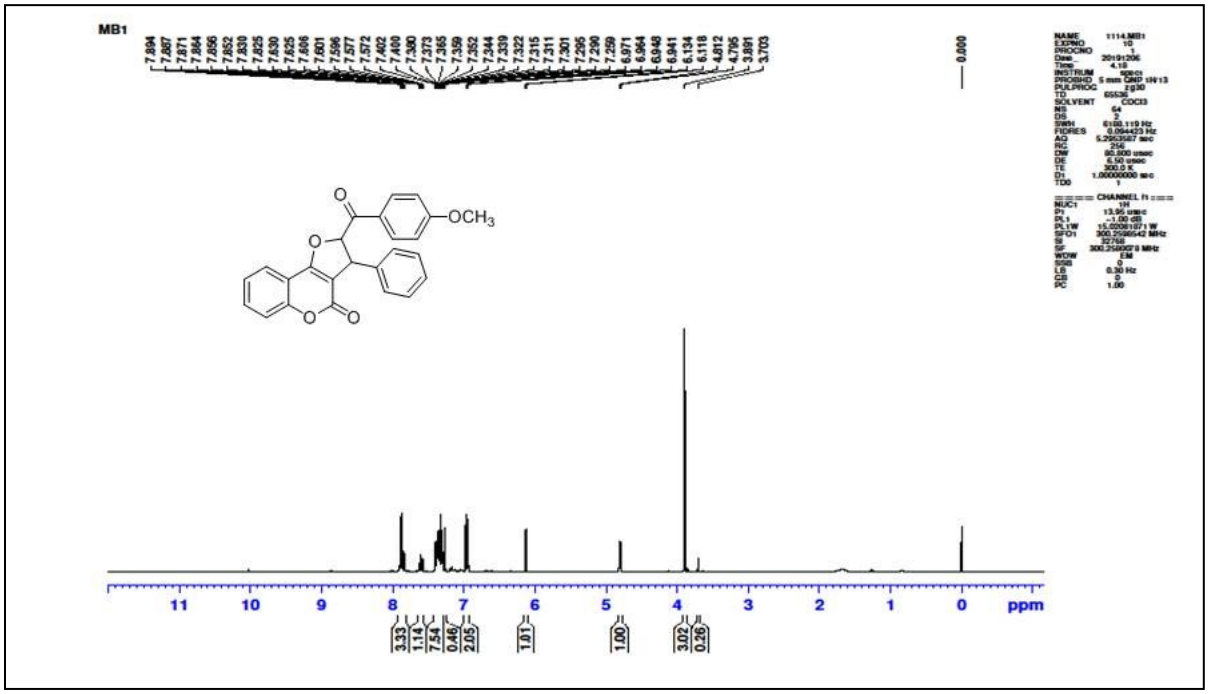

^{13}CNMR of Compound (4c)

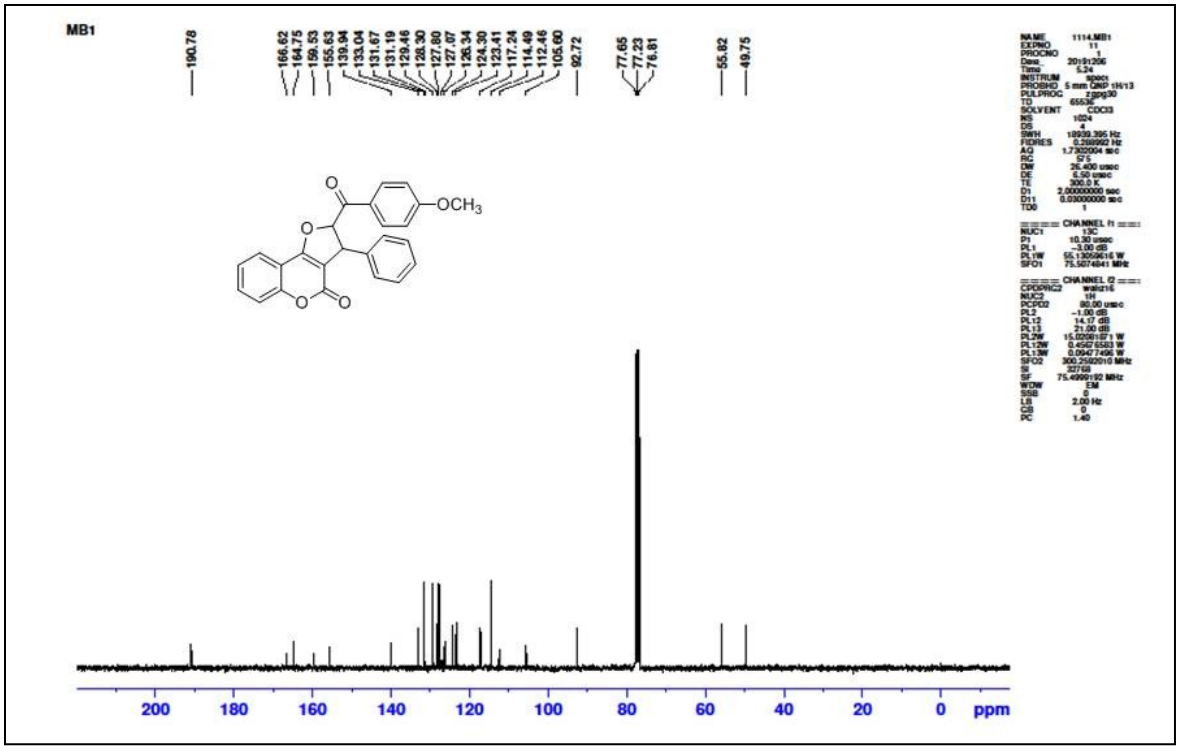

^{1}HNMR of Compound (4f)

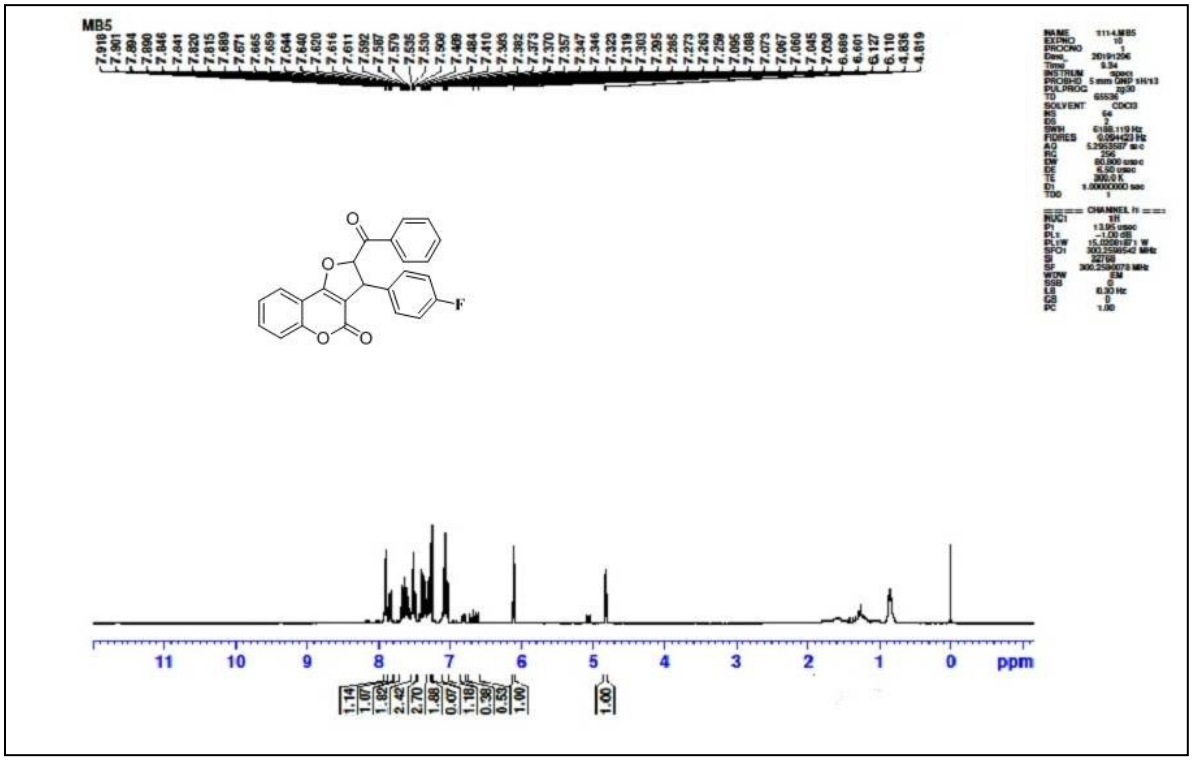

[1]HNMR of Compound (4g)

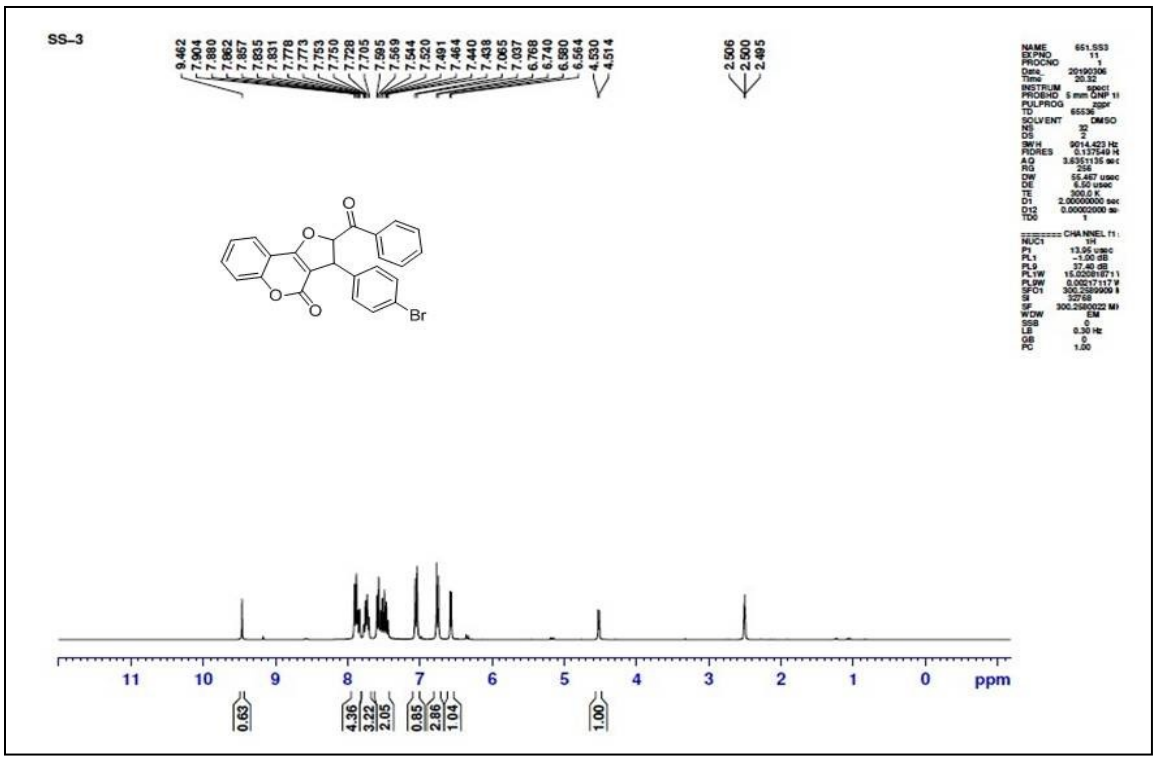

[1]HNMR of Compound (4h)

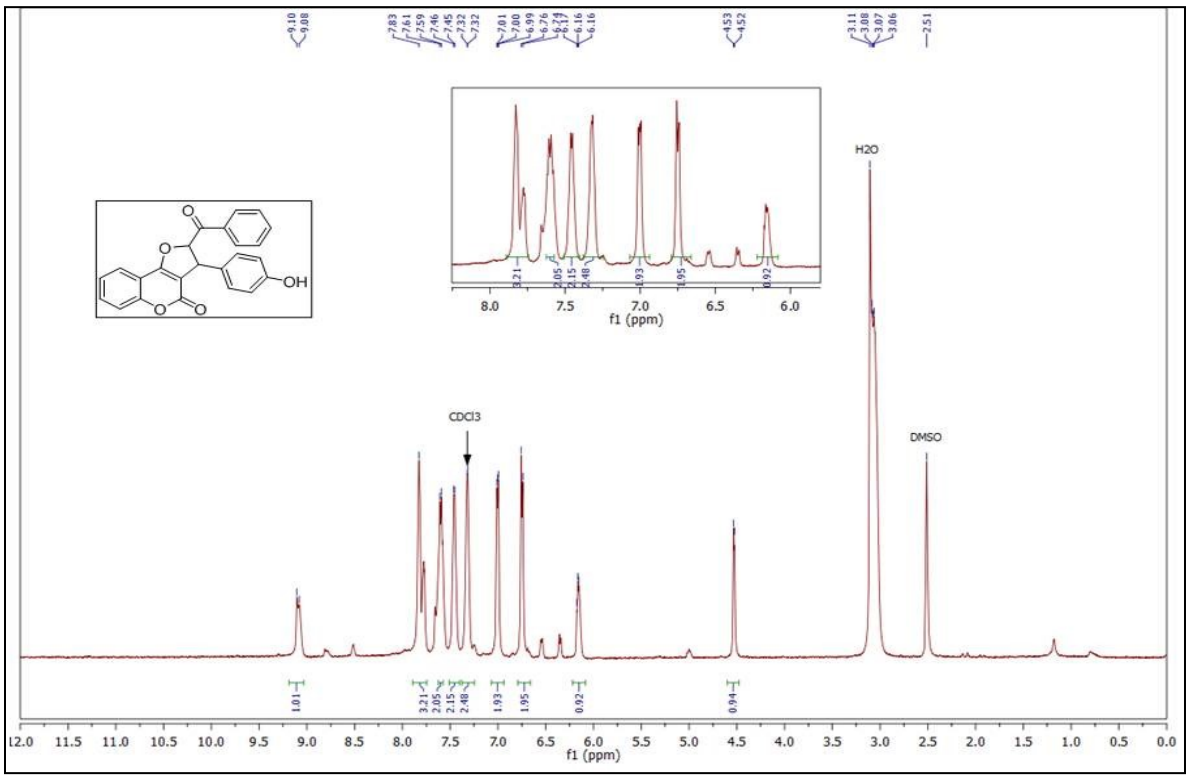

^{13}CNMR of Compound (4h)

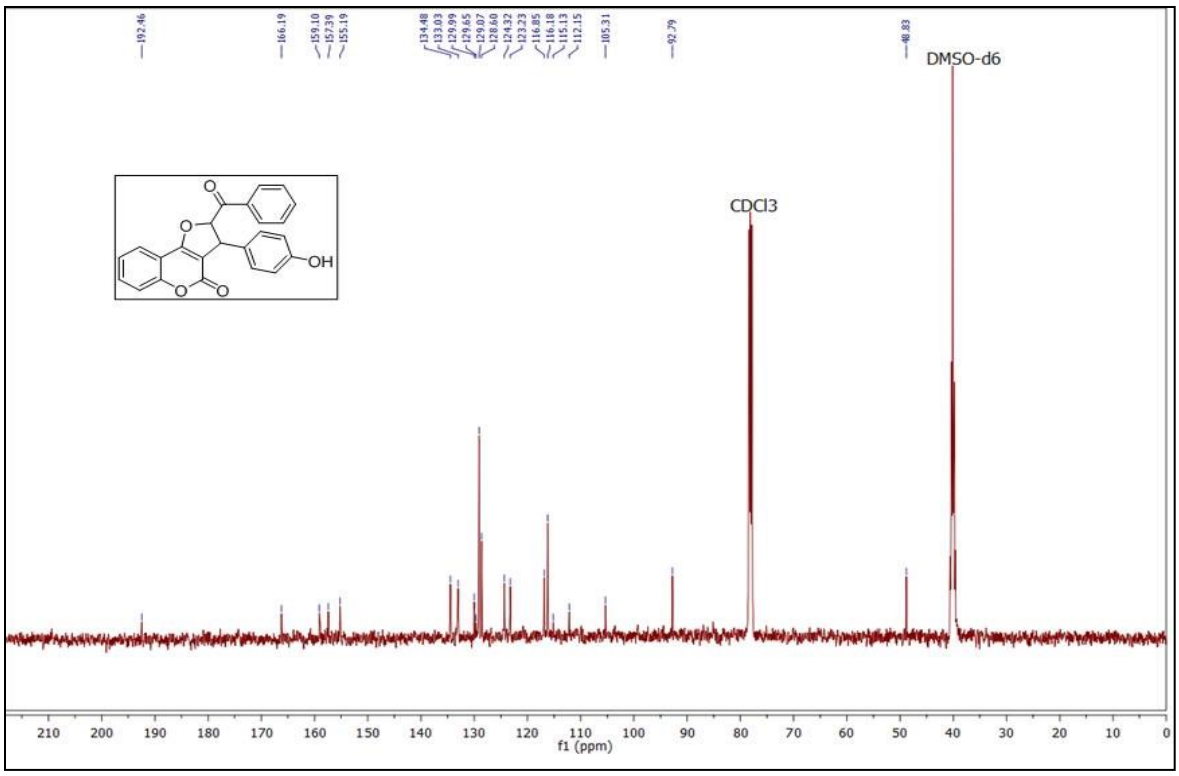

^{1}HNMR of Compound (4j)

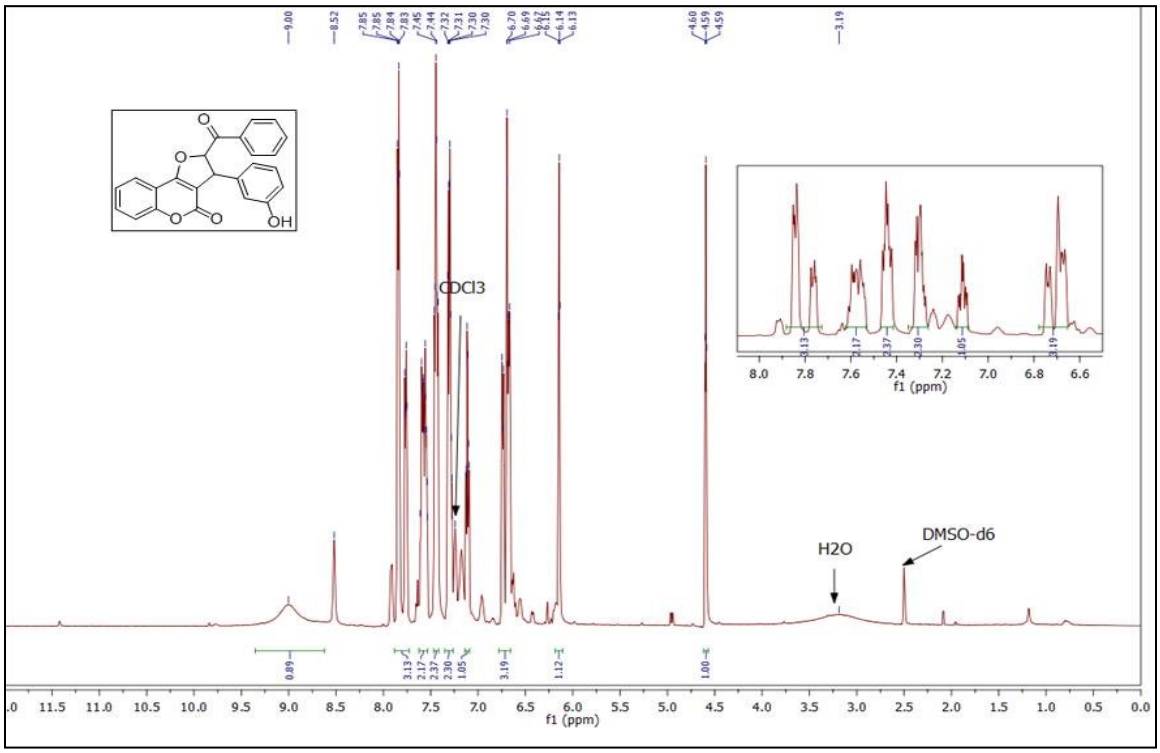

^{13}CNMR of Compound (4j)

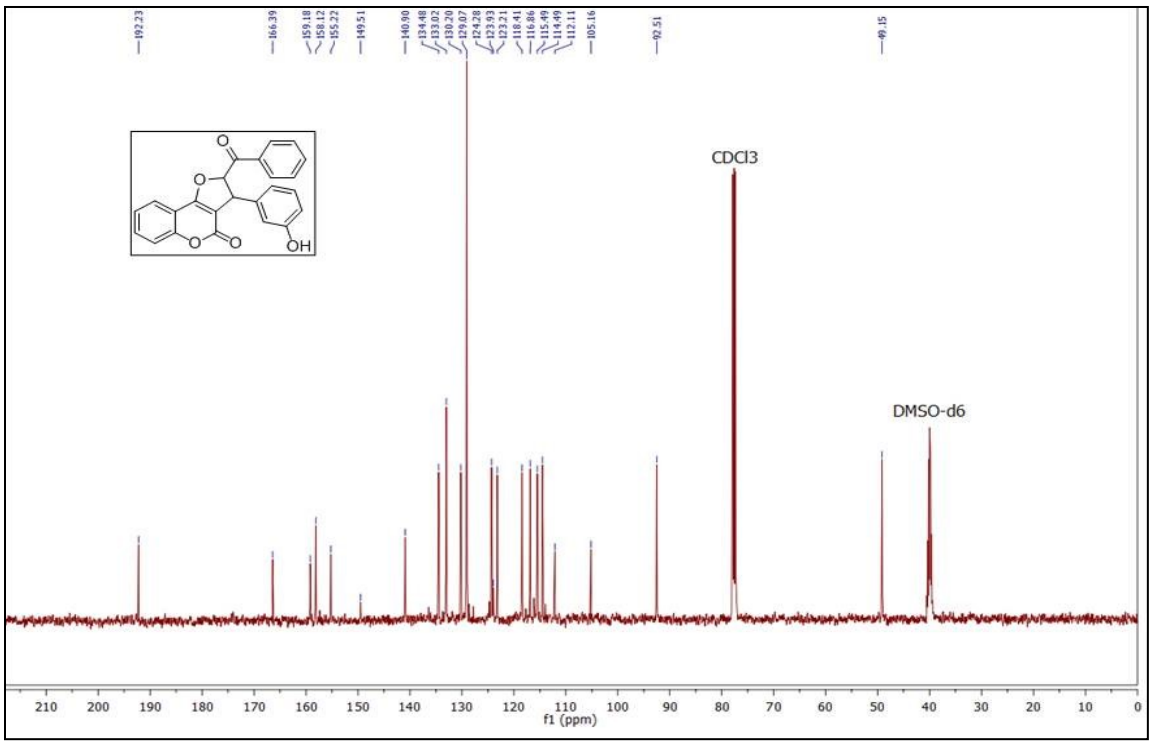

^{1}HNMR of Compound (4o)

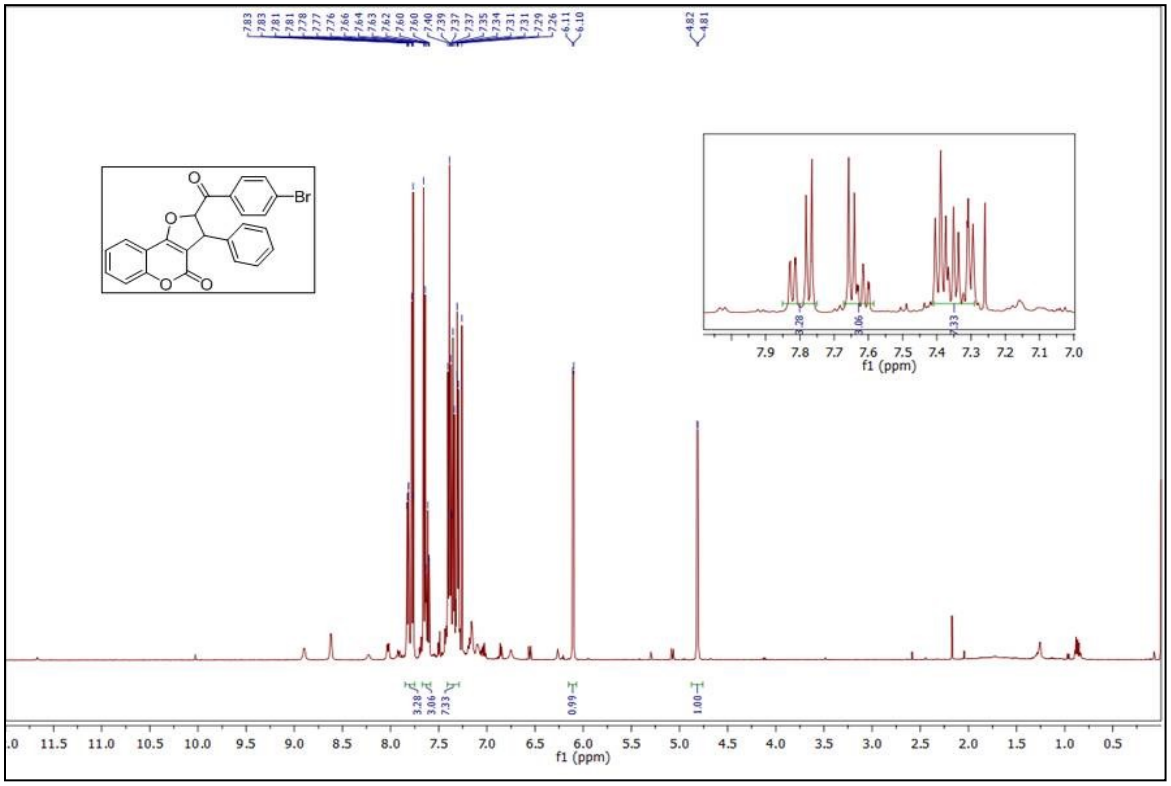

^{13}CNMR of Compound (4o)

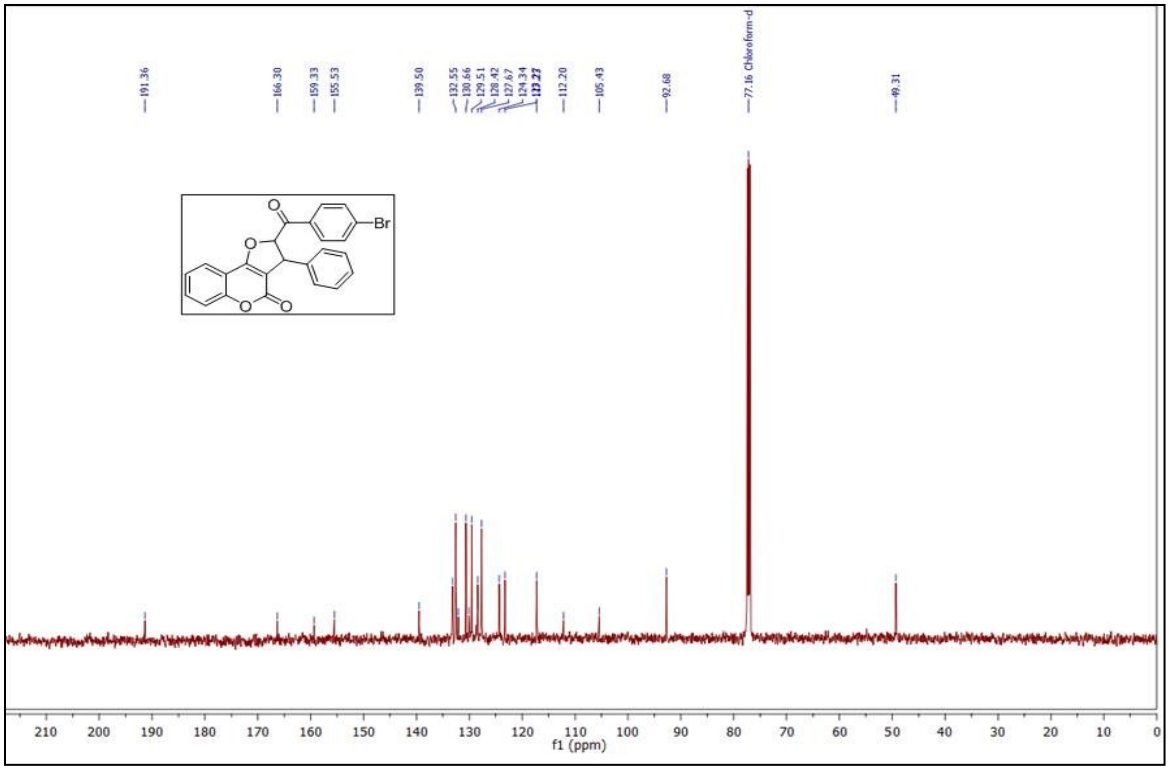

^{1}HNMR of Compound (4p)

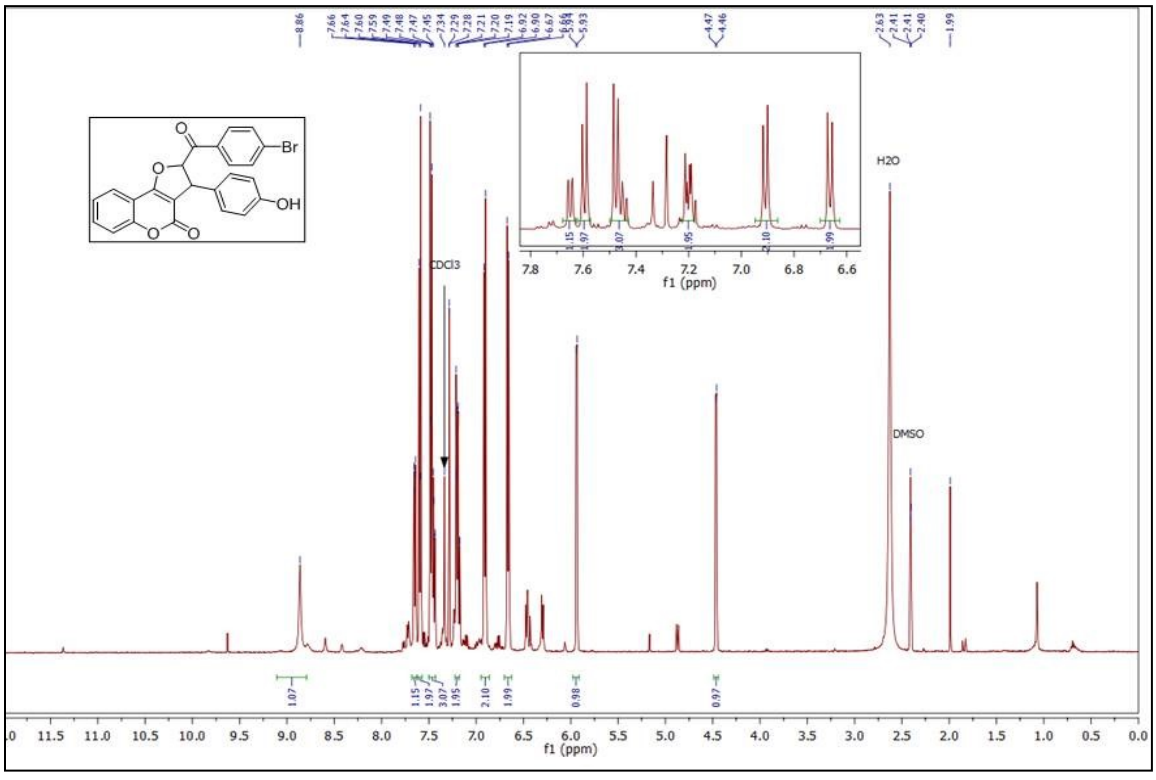

^{13}CNMR of Compound (4p)

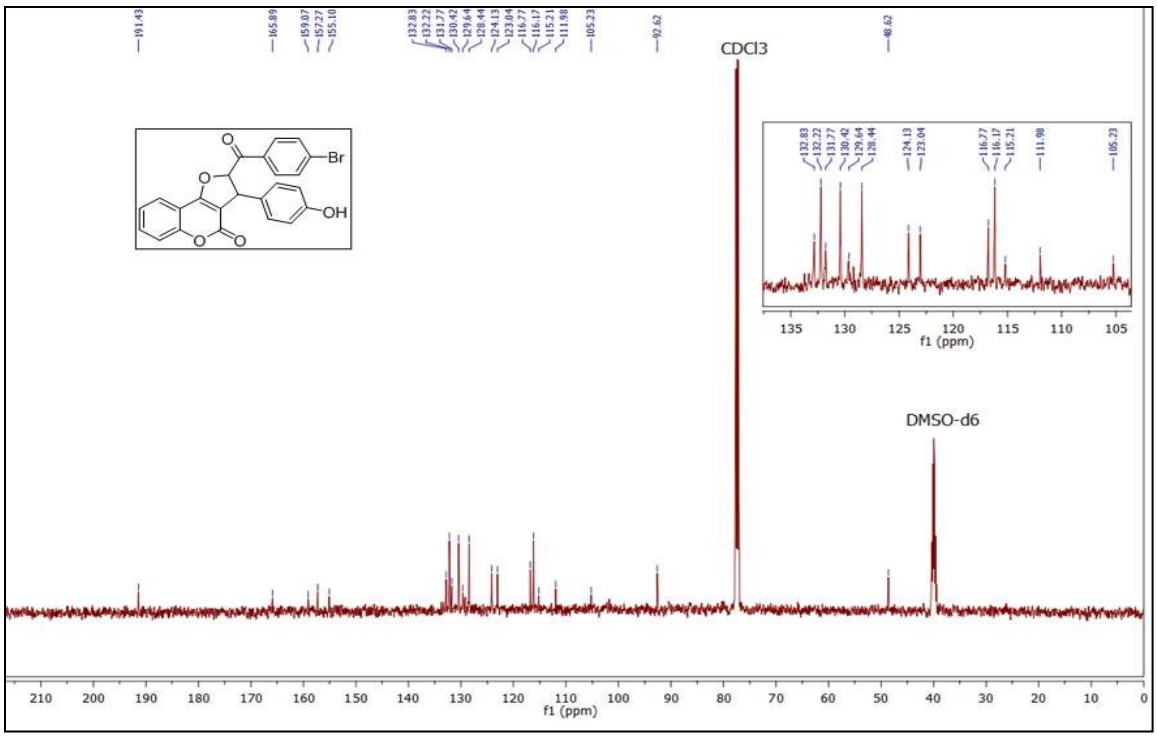

^{1}HNMR of Compound (4r)

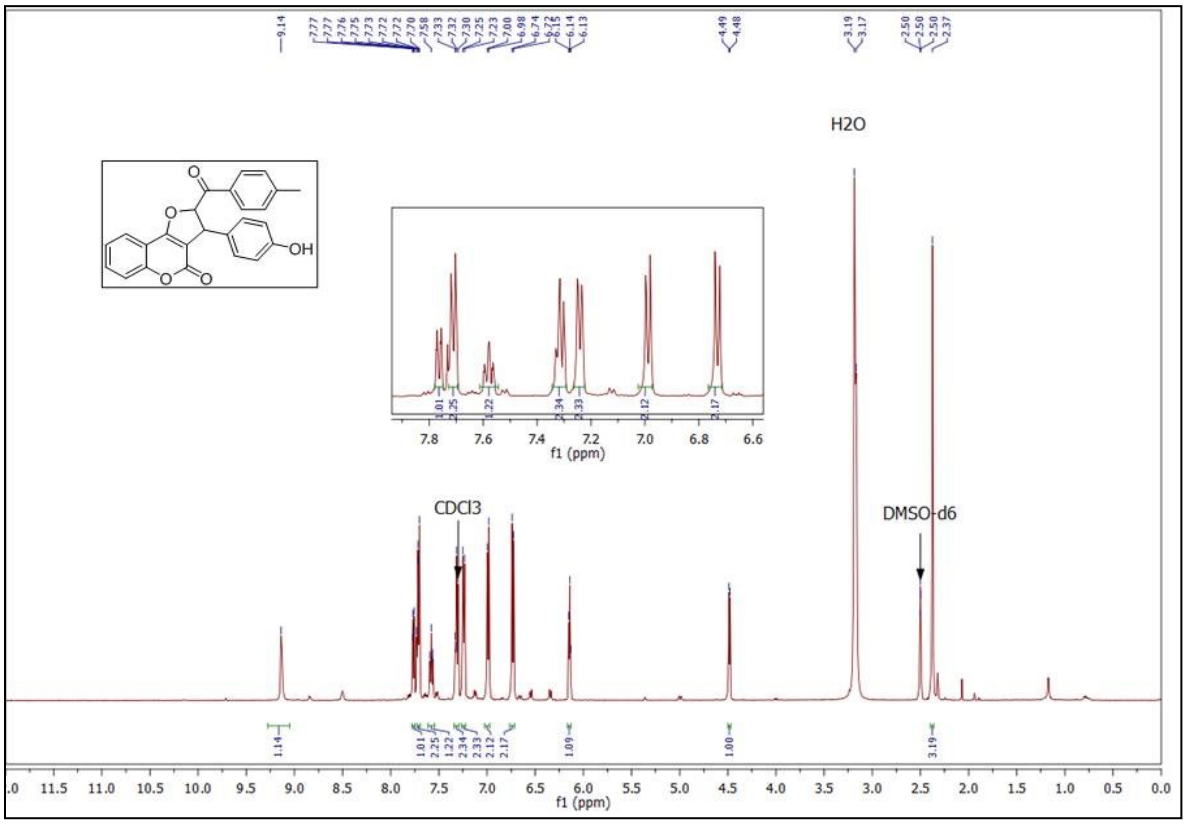

[13]CNMR of Compound (4r)

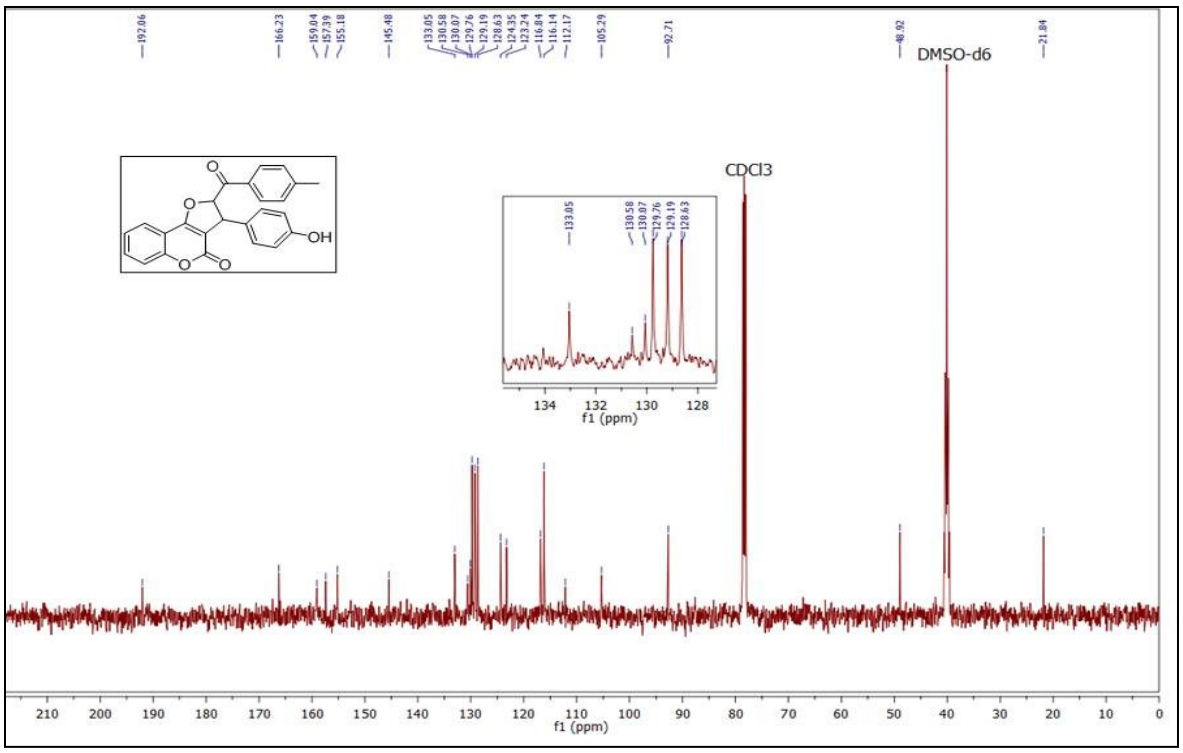

[1]HNMR of Compound (4t)

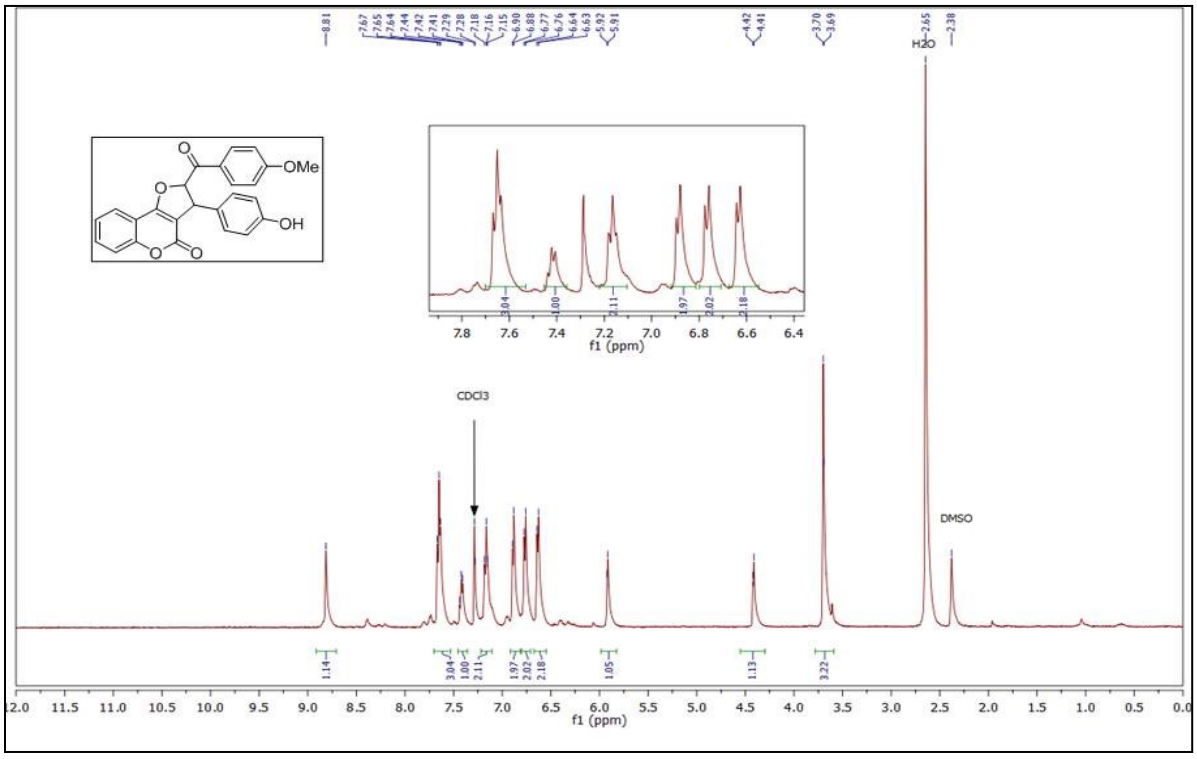

^{13}CNMR of Compound (4t)

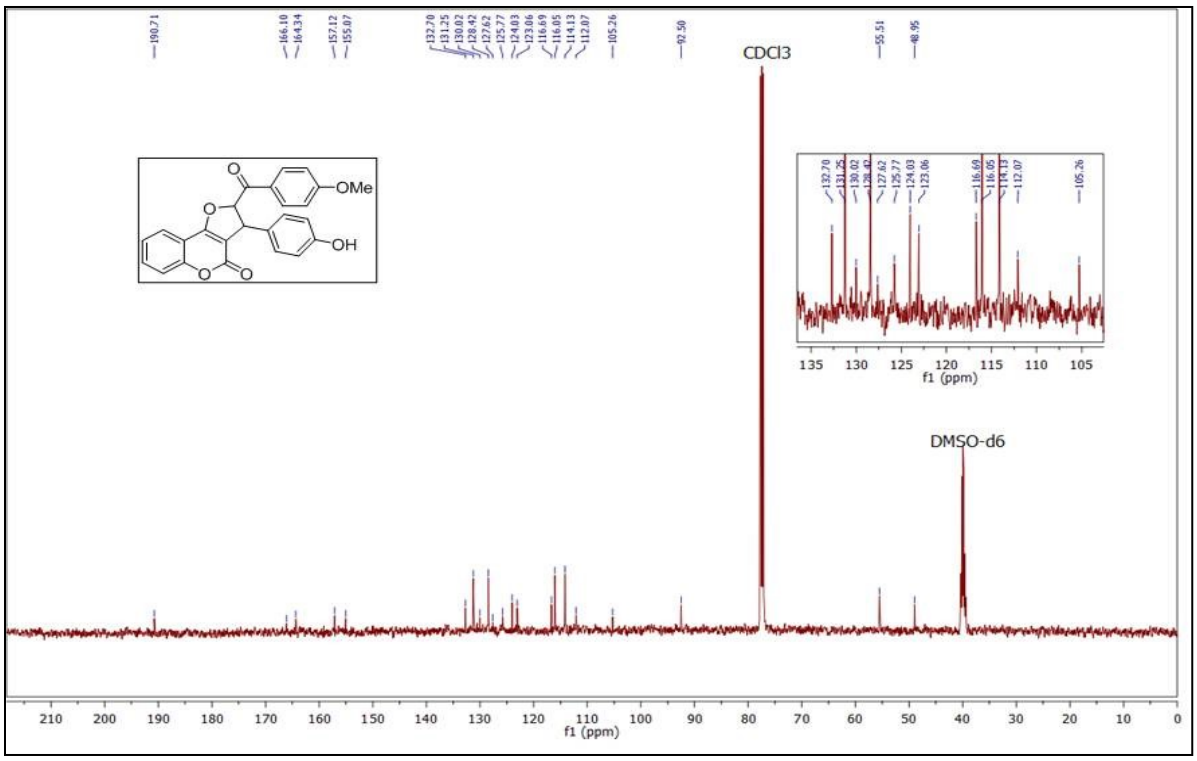

Supplementary Data for *in silico* pharmacophore based target screening of DHFC derivatives:

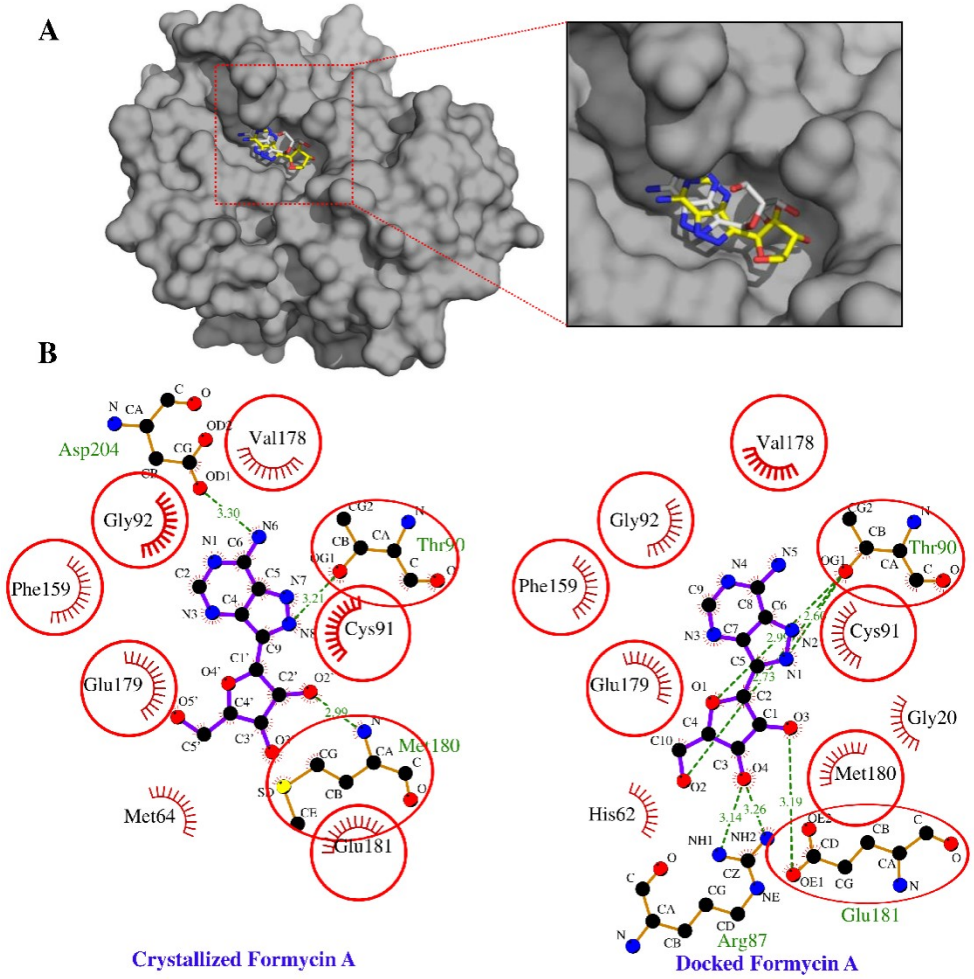

Supplementary Fig.1: Fidelity of the docking protocol. (A) & (B) represent the comparative analysis of co-crystallized (represented as white carbon sticks) and docked (represented as yellow carbon sticks) conformations of FormycinA at the active site catalytic cleft of *Trichomonas vaginalis* Purine nucleoside phosphorylase in the three dimensional and two dimensional interaction layouts respectively.

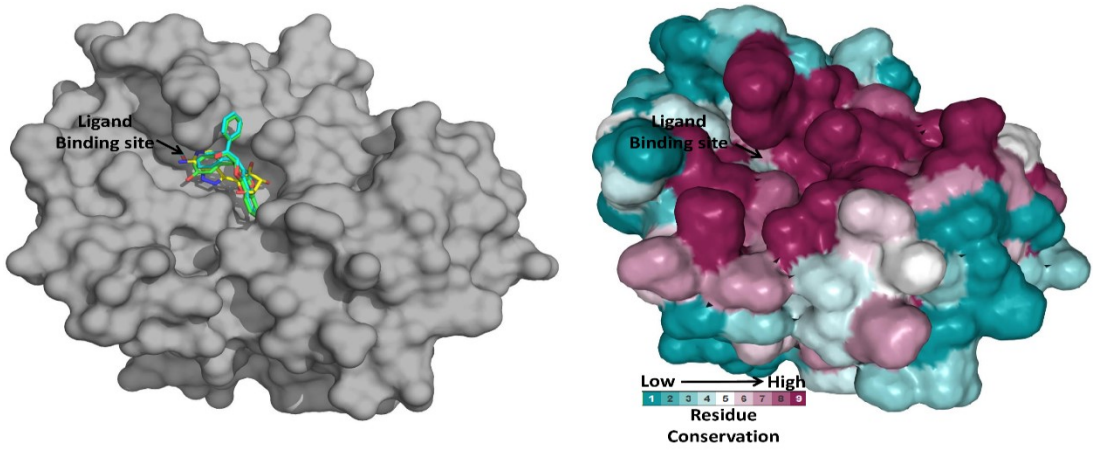

Supplementary Fig.2: FormycinA (represented as yellow carbon sticks) and DHFC derives **4c** and **4j** (represented as cyan and green carbon sticks respectively) share the same highly conserved catalytic cleft of *Trichomonas vaginalis* Purine nucleoside phosphorylase.

Supplementary Table 1: Binding energy ($\Delta G_{binding}$) estimation of synthesized *trans*-2,3-dihydrofuro[3,2-c] coumarin (DHFC) derivatives with *Trichomonas vaginalis* Purine nucleoside phosphorylase through *in silico* molecular docking analysis.

S.No.	Compounds Name	Binding Energy (Kcal/Mol)	pK_d(-logK_d)
1	**4a**	-9.1	5.5
2	**4b**	-8.6	4.61
3	**4c**	-9.6	5.98
4	**4d**	-9	5.54
5	**4e**	-9.3	5.62
6	**4f**	-9.4	6.01
7	**4g**	-7.9	5.61
8	**4h**	-8.4	4.82
9	**4i**	-8.7	5.18
10	**4j**	-9.2	5.91
11	**4k**	-7.8	4.57
12	**4l**	-8.3	5.22
13	**4m**	-7.8	4.99
14	**4n**	-8.3	5.36

15	**4o**	-9.4	6.48
16	**4p**	-9.1	6.29
17	**4q**	-8.9	5.61
18	**4r**	-8.8	5.68
19	**4s**	-8.7	5.94
20	**4t**	-8.8	5.9

Materials and Methods:

***In silico* pharmacophore based therapeutic target screening of DHFC derivatives**

Initially the synthesized DHFC derivatives were screened to identify the biological target of importance through *in silico* pharmacophore based reverse docking approach.[3] Initial reverse docking results indicated purine nucleoside phosphorylase of *Trichomonas vaginalis* (TvPNP)[4] could be a potential target protein of the synthesized ligands. To further test the results obtained through initial reverse docking approach, AutoDock vina an application that uses Lamarkian Genetic Algorithm was used to perform receptor based molecular docking[5] of the synthesized DHFC derivatives. Crystal structure of *Trichomonas vaginalis* purine nucleoside phosphorylase (TvPNP) was downloaded from PDB (PDB ID: 1Z33),[6,7] water, ligands and other non-bonded molecules were deleted by using PyMol.[8] Polar hydrogen and Kollman charges were added to receptor protomer using molecular graphic laboratory tools (MGL Tools).[9]

Again the same tools were used to fix the number of rotatable bonds of the ligand molecules. Blind docking was performed individually to all synthesized DHFC ligands with TvPNP using grid box size (44Å, 58Å and 54Å with the grid spacing of 1Å). Out of nine poses, best pose of the ligands was considered as it has the minimum root mean square deviation (RMSD) and minimum free energy of binding ($\Delta G_{Binding}$). Interaction profile of all the ligands with TvPNP receptor was analysed by using PyMol and LigPlot.[12] We have compared the binding sites of our ligands with already solved crystal structure of TvPNP with substrate and inhibitors (PDB ID: 1Z34 and 1Z36 respectively).[7] Further we were interested to calculate the affinity of the ligands with TvPNP receptor. To accomplish affinity prediction we have used KDEEP, a deep learning based online web server.[11]

Furthermore, to predict the stability of the ligand protein interaction we have performed the molecular dynamic simulation using NAMD.[13] Protein and protein ligand docked complexes were individually subjected for molecular dynamic simulation for a total simulation time of 30ns. To generate parameters and topology files we have used online platform CHARMM-GUI.[14,15] Visual molecular dynamic (VMD) was applied to generate the PSF files for protein ligand complex and free protein. Solvation was done with 5Å boundary of cubic water for free protein as well as docked ligand protein complexes and langevin dynamics was used to set isothermal-isobaric ensemble environment. Frequencies for restart and dcd were kept for 3000 steps. Steepest descent methods were used for energy minimization for 1000 steps and to calculate interactions of non-bonded atoms a cutoff was set to 10Å. 2 fs was set time step throughout whole simulation. To calculate the electrostatic interactions the Particle Mesh Ewald (PME) method was used. All simulations were performed for 30 ns. The simulated RMSD trajectory was analyzed by VMD software. Root Mean square Deviation (RMSD) trajectory over simulation time for only protein and protein ligand complexes were visualized through VMD and compared to predict the stability of the protein ligand complexes throughout the entire length of simulations.

Amino acid conservation score over the course of evolution has been predicted using ConSurf server[13] to estimate the mutability of the ligand binding surfaces which might indicate the future emergence of ligand binding recalcitrance and drug resistance. Accordingly the colour coded surface of the protein (TvPNP) has been represented highlighting the highly conserved ligand binding cleft. All the structural representations were prepared by using PyMol and the graphs were prepared by using OriginLab (https://www.originlab.com/)

References Materials and Methods:

1. Y. Tangella, K. L. Manasa, V. L. Nayak, M. Sathish, B. Sridhar, A. Alarifi, N. Nagesh, A. Kamal, An efficient one-pot approach for the regio- and diastereoselective synthesis of trans-dihydrofuran derivatives: cytotoxicity and DNA-binding studies. *Org. Biomol. Chem*., 2017, **15**, 6837-6853.
2. J. Safaei-Ghomi, H. Shahbazi-Alavi, P. Babaei, One-pot multicomponent synthesis of furo[3,2-*c*]coumarins promoted by amino functionalized Fe_3O_4@SiO_2 nanoparticles. *De Gruyter* Z. Naturforsch. 2016; **71(8)b**, 849-856.

3. W. Xia, S. Yihang, W. Shiwei, L. Shiliang, Z. Weilin, L. Xiaofeng, L. Luhua, P. Jianfeng, L. Honglin, PharmMapper 2017 update: a web server for potential drug target identification with a comprehensive target pharmacophore database. *Nucleic Acids Res.* 2017**, 45(1)**, 356-360.
4. N. Munagala, C. W. Ching, The purine nucleoside phosphorylase from *Trichomonas vaginalis* is a homologue of the bacterial enzyme. *Biochemistry* 2002, **41(33)**, 10382-10389.
5. A. R. Allouche, Gabedit a graphical user interface for computational chemistry softwares. *J. Comput. Chem*. 2011, **32(1)**, 174-182.
6. M. B. Helen, W. John, F. Zukang, G. Gary, T. N. Bhat, W. Helge, N. S. Ilya, E. B. Philip, The Protein Data Bank. *Nucleic Acids Res*. 2000, **28(1)**, 235-242.
7. Y. Zang, W. H. Wang, S. W. Wu, S. E. Ealick, C. C. Wang, Identification of a subversive substrate of *Trichomonas vaginalis* purine nucleoside phosphorylase and the crystal structure of the enzyme-substrate complex. *J. Biol. Chem*. 2005, **280(23)** 22318-22325.
8. L. Schrödinger, W. DeLano, The PyMOL Molecular Graphics System, Version 2.4.0, Schrodinger, LLC.
9. G. Morris, R. Huey, W. Lindstrom, M. Sanner, R. Belew, D. Goodsell, A. Olson, Autodock 4 and Auto Dock Tools 4: automated docking with selective receptor flexiblity. *J. Comput. Chem*. 2009, **30(16)**, 2785-91.
10. A. C. Wallace, R. A. Laskowski, J. M. Thornton, LIGPLOT: a program to generate schematic diagrams of protein-ligand interactions. *Protein Eng.* 1995, **8(2),** 127-134.
11. J. Jiménez, M. Skalic, G. Martinez-Rosell, G. K. De Fabritiis, deep: protein-ligand absolute binding affinity prediction via 3d-convolutional neural networks. *J. Chem. Inf. Model*. 2018, **58(2)**, 287-296.
12. J. C. Phillips, D. J. Hardy, J. D. C. Maia, J. E. Stone, J. V. Ribeiro, R. C. Bernardi, R. Buch, G. Fiorin, J. Henin, W. Jiang, R. McGreevy, M.C. R. Melo, B. K. Radak, R. D. Skeel, A. Singharoy, Y. Wang, B. Roux, A. Aksimentiev, Z. Luthey-Schulten, L. V. Kale, K. Schulten, C. Chipot, E. Tajkhorshid, Scalable molecular dynamics on CPU and GPU architectures with NAMD. *J. Chem. Phys*. 2020, **153 (4)**, 044130.

13. S. Jo, T. Kim, V. G. Iyer, W. Im, CHARMM-GUI: a web-based graphical user interface for CHARMM. *J. Comput. Chem*. 2008, **29(11)**, 1859-1865.
14. S. Kim, J. Lee, S. Jo, C. L. Brooks, H. S. Lee, W. Im, CHARMM-GUI ligand reader and modeler for CHARMM force field generation of small molecules. *J. Comput. Chem*. 2017, **38 (21)**, 1879-1886.
15. H. Ashkenazy, S. Abadi, E. Martz, O. Chay, I. Mayrose, T. Pupko, N. Ben-Tal Con Surf 2016: an improved methodology to estimate and visualize evolutionary conservation in macromolecules.*Nucl. Acids Res.* 2016, **44(1)**, 344-350.